Microbiome

RESEARCH

Open Access

Multi-site microbiota alteration is a hallmark of kidney stone formation

Kait F. Al[1,2], Benjamin R. Joris[3], Brendan A. Daisley[4], John A. Chmiel[1,2], Jennifer Bjazevic[5], Gregor Reid[1,2,5], Gregory B. Gloor[3], John D. Denstedt[5], Hassan Razvi[5] and Jeremy P. Burton[1,2,5*]

Abstract

Background Inquiry of microbiota involvement in kidney stone disease (KSD) has largely focussed on potential oxalate handling abilities by gut bacteria and the increased association with antibiotic exposure. By systematically comparing the gut, urinary, and oral microbiota of 83 stone formers (SF) and 30 healthy controls (HC), we provide a unified assessment of the bacterial contribution to KSD.

Results Amplicon and shotgun metagenomic sequencing approaches were consistent in identifying multi-site microbiota disturbances in SF relative to HC. Biomarker taxa, reduced taxonomic and functional diversity, functional replacement of core bioenergetic pathways with virulence-associated gene markers, and community network collapse defined SF, but differences between cohorts did not extend to oxalate metabolism.

Conclusions We conclude that multi-site microbiota alteration is a hallmark of SF, and KSD treatment should consider microbial functional restoration and the avoidance of aberrant modulators such as poor diet and antibiotics where applicable to prevent stone recurrence.

Keywords Microbiota, Kidney stones, Gut microbiota, Urinary microbiota, Shotgun metagenomic sequencing, Urology

Background

Kidney stone disease, or nephrolithiasis, is a prevalent condition that causes significant morbidity to sufferers and is a draining financial burden to healthcare systems [1]. Although traditionally considered to be an affliction of obese and middle-aged men, prevalence has risen in recent decades, specifically in young women and children [2–5]. The human microbiota is known for its role in systemic health and disease, including metabolic syndrome, cardiovascular disease, and diabetes [6–8]. All of these conditions are comorbidities associated with nephrolithiasis, and their increasing prevalence over recent years along with that of stone disease indicate systemic declines in our population's overall health. Importantly, the human microbiota is also implicated in nephrolithiasis, but a consensus on the mechanisms behind this relationship remains elusive.

Calcium oxalate (CaOx) is the most common crystalline composition of stones, followed by calcium phosphate, uric acid, struvite, and cystine [9]. Oxalate is a toxic terminal metabolite produced endogenously, while a smaller portion is consumed in the diet [10]. *Oxalobacter formigenes* (now also *O. aliiformigenes*,

*Correspondence:
Jeremy P. Burton
Jeremy.burton@lawsonresearch.com
[1] Centre for Human Microbiome and Probiotic Research, Lawson Health Research Institute, London, ON, Canada
[2] Department of Microbiology and Immunology, The University of Western Ontario, London, ON, Canada
[3] Department of Biochemistry, The University of Western Ontario, London, ON, Canada
[4] Molecular and Cellular Biology Department, University of Guelph, Guelph, ON, Canada
[5] Division of Urology, Department of Surgery, The University of Western Ontario, London, ON, Canada

O. paeniformigenes, and *O. paraformigenes*) [11] was thought to be a key modulator of oxalate in the human body — it utilizes the molecule as its sole carbon source, and some studies have shown that intestinal colonization with this bacterium may be associated with lower urinary oxalate levels and subsequently a lower risk of developing CaOx stones [12, 13]. However, other members of the gut microbiota are also capable of degrading oxalate [14, 15], and many recent studies have found no difference in colonization rates of *O. formigenes* between healthy persons and stone formers [16–21]. Thus, it remains unclear if direct oxalate metabolism by gut colonizers is the key to preventing kidney stones.

Beyond oxalate utilization, previous studies have demonstrated generalized "dysbiosis" in the intestinal microbiota of kidney stone formers [16–18, 20–26]. However, the significant perturbations determined in these studies are seldom consistent; this may be an artifact of small sample size, or different sequencing and analysis methodologies. Most of the studies to date have also focused primarily on the presence or absence of *O. formigenes* and direct oxalate utilization pathways, but the narrow focus towards these analyses may be overemphasizing their true functional significance to the disease pathology.

Except for infection, the urinary system was historically believed to be sterile; however, a urinary microbiota in healthy humans has been well described in the last decade [27, 28]. This discovery has led investigators to question the role microbes may play in nephrolithiasis [29]. Indeed, while struvite stones are known to be associated with urinary tract infections (UTI), recent culture-dependent and culture-independent studies have also confirmed the presence of bacteria in calcium-based stones [16, 30, 31]. Recent evidence suggests that direct bacterial oxalate utilization could also play a role in the urinary tract [32], but much is still unknown about how resident bacteria may be contributing to the disease, and whether stone-bound microbes result from an aberrant urinary or gut microbiota. Which body site is of most significance to the pathology is still unclear, and an untargeted holistic role for the microbiome beyond direct oxalate utilization has been underexplored.

The aim of the present study was to comprehensively characterize the urinary and gut microbiota of kidney stone formers (SF) and healthy controls (HC) to assess body site-specific microbial contributions to nephrolithiasis. The distant site of the oral cavity was also explored due to its known associations with systemic disease [33]. It was anticipated that this would provide insights into the role of bacteria from multiple body sites in stone formation, and foundational knowledge upon which personalized medicine and targeted therapies could be developed for the prevention and treatment of nephrolithiasis.

Methods

Patients and sample collection

Eighty-three active nephrolithiasis patients (SF) were recruited from the Urology Department at St. Joseph's Hospital in London, Ontario, along with thirty healthy control participants (HC) between August of 2015 and January of 2019. Ethical approval for the KiSMi study was granted by Lawson Health Research Institute (CRIC R 15–117) and the Health Sciences Research Ethics Board at the University of Western Ontario (REB #105443) in London, Ontario. Written consent was obtained from all the study participants at the time of study inclusion and the methods were carried out in accordance with the approved guidelines. Inclusion and exclusion criteria for the participants are provided in Supplementary Table 1. Briefly, neither HC nor SF could have an active gastrointestinal infection or antibiotic exposure within the 30 days prior to study enrollment (although in actuality all participants had at least 90 days without antibiotic exposure, an acceptable criterion based on current literature [34]). Additionally, HC could not have inflammatory bowel disease, a history of gastric bypass surgery, a history of urosepsis in the past year, a urinary diversion, an indwelling catheter, or intermittent catheterization performed. In comparison, the SF were still eligible to be included with these health issues, but only three SF had IBD (which was accounted for in multivariate analyses, Supplementary Data), and the other conditions were not present in any SF. All SF patients who met the inclusion criteria were recruited during regularly scheduled clinic appointments prior to their ureteroscopy (URS) or percutaneous nephrolithotomy (PCNL) for stone removal; HC subjects were approached in the community, and age and sex matched to SF with a loose frequency-matching approach [35].

Sample processing and DNA extraction

Upon recruitment, participants were asked about relevant demographic and medical history including antibiotic usage and their history of urinary tract infections (Table 1, Supplementary Data 1A). Following enrolment, HC were evaluated by ultrasound to confirm stone-free status. All participants then provided a midstream urine sample, oral saliva swab, and 102 out of 113 mailed in a fecal sample on toilet paper [36]. They also completed a validated food frequency questionnaire based on estimated yearly intake and portion size to provide daily nutrient estimates [37]. During surgical stone removal, additional clinical samples were collected from SF where possible: urine, upon first

insertion of the catheter and prior to instilling saline into the urinary tract, and stone fragments from PCNL. Prophylactic antibiotics were administered peri-operatively, differentiating the operating room (OR) urine and stone samples from all other specimens collected. In the majority of cases, patients undergoing PCNL had 5 days of oral ciprofloxacin pre-operatively, followed by IV ampicillin and gentamycin in the OR and then for 24 h after surgery. URS patients would typically receive IV cefazolin in the OR and were then discharged home with a 3–5-day course of trimethoprim/sulfamethoxazole or ciprofloxacin. These OR specimens were placed by the surgeon into a sterile collection cup. An OR environmental control sample was also collected where a sterile urine container containing 200 µL of nuclease-free water was left open beside the patient for the duration of their surgery. The composition of additional available stone fragments was analysed by the St. Joseph's Healthcare Toxicology and Special Chemistry Lab by Fourier transform infrared spectrophotometry.

All urine samples (i.e. from HC as well as pre-operative and OR urine from SF) were processed in two portions within 2 h of collection. Where possible, 10 mL of whole urine was collected and frozen at − 80 °C for high-performance liquid chromatography (HPLC) analyses of urinary metabolites. The remainder was processed as previously described [38, 39] and stored for future 16S rRNA gene sequencing. Briefly, the entire remaining volume of urine was centrifuged for 10 min at 5000 × *g*, after which the supernatant was decanted off and the pellet was stored dry at − 80 °C until DNA extraction. If the total urine volume was under 25 mL, only 2 mL of whole urine was reserved for HPLC. The urine volume that resulted in the pellet for 16S rRNA gene sequencing was recorded to identify confounding factors in the downstream sequencing analysis associated with processing conditions.

Oral swabs were frozen at − 80 °C within 2 h of their initial collection and stored for future DNA extraction and 16S rRNA gene amplicon sequencing. In a validated method adapted from the American Gut Project [36, 40, 41], fecal samples were collected by participants at home and mailed to the laboratory, where they were frozen at − 80 °C within 2 h of their receipt. Within 2 h of collection, the water inside the OR environmental control sample was shaken in the cup for 2 min and the entire volume was transferred to a PCR-grade Eppendorf tube and frozen at − 80 °C.

Within 2 h of their initial collection, one stone fragment per patient was transferred to a PCR-grade Eppendorf tube and frozen at − 80 °C.

For DNA extraction, urine, stone, and OR environmental control samples were randomized across 96-well extraction plates together; oral and fecal samples were extracted on separate plates to mitigate potential contamination to the other samples which were of lower biomass in comparison.

Samples were thawed and processed in a sterile biosafety hood. Using tweezers sterilized with RNase AWAY™, the kidney stone was transferred to a sterile cell strainer mounted onto an empty 50-mL conical tube. New sterile cell strainers and conical tubes were used for every sample. Two milliliters of nuclease-free water was gently rinsed over the external surface of the stone. The stone was then transferred to a mortar and pestle that was sterilized with 5% sodium hypochlorite followed by RNase AWAY™ and pulverized into sand-like fragments. The fragments were suspended in 100 µL of nuclease-free water and pipetted directly into wells of the bead plate of the DNeasy PowerSoil HTP 96 Kit utilized for DNA extraction. Urine pellets were thawed and suspended in 100 µL of nuclease-free water, then pipetted into the bead plate. The 100 µL OR environmental control water sample was transferred directly to the bead plate. Oral swabs were cut directly into the wells of the bead plate with RNase AWAY™-treated scissors. Toilet paper samples were dissected and trimmed with RNase AWAY™-treated scissors and forceps such that a piece of visibly soiled paper approximately 1 cm^2 in size was added directly to the bead plate.

Two wells in every plate were left empty and acted as negative controls. Two positive controls, or spikes, were added to each plate and were 100 µL of pure bacterial culture: Spike 1 was *Escherichia coli* strain DH5α, and Spike 2 was *Staphylococcus aureus* strain Newman. For preparation of the spikes, a single colony of the bacteria was inoculated into 10 mL of Luria–Bertani (LB) broth and grown overnight at 37 °C. One hundred-microlitre aliquots of the overnight cultures were portioned into 1.5-mL Eppendorf tubes and frozen at − 80 °C. For each DNA extraction plate, a single tube of both spikes was thawed and pipetted directly into the PowerSoil HTP bead plate with PCR-grade filter tips. DNA was isolated from samples using the DNeasy PowerSoil HTP 96 Kit according to the manufacturer's instructions with minor adjustments as described previously [38]. DNA was stored at − 20 °C until PCR amplification.

16S rRNA gene sequencing of urine, stone and oral swab samples

PCR amplification was completed using the Earth Microbiome universal primers, 515F and 806R, which are specific for the V4 variable region of the 16S rRNA gene [42]. Primers and barcode sequences are listed in Supplementary Table 2. PCR reagent set-up was performed using a Biomek® 3000 Laboratory Automation Workstation

(Beckman-Coulter, Mississauga, ON, CAN). Ten microlitres of each left- and right-barcoded primers (3.2 pMole/μL) was arrayed in 96-well plates such that each well contained a unique combination of left and right barcodes. Two microlitres of DNA template was added to the primer plate, followed by 20 μL of Promega GoTaq hot-start colourless master mix. The reaction was briefly mixed by pipetting, then plates were sealed with foil plate covers and centrifuged for 2 min at room temperature at 2250 × *g*.

Amplification was carried out using an Eppendorf thermal cycler (Eppendorf, Mississauga, ON, CAN), where the lid temperature was maintained at 104 °C. An initial warm-up of 95 °C for 4 min was utilized to activate the GoTaq, followed by 25 cycles of 1 min each of 95, 52, and 72 °C. Sequencing was carried out at the London Regional Genomics Centre (http://www.lrgc.ca; London, ON, CAN). Amplicons were quantified using pico green and pooled at equimolar concentrations before cleanup. Using the 600-cycle MiSeq Reagent Kit, paired-end sequencing was carried out as 2 × 260 cycles with the addition of 5% ϕX-174 at a cluster density of ~ 1100. Reads were exported as fastq files (uploaded to NCBI Sequence Read Archive, BioProject ID PRJNA856314 (urinary) and PRJNA856641 (oral). Reads were demultiplexed using Cutadapt [43], quality filtered utilizing the DADA2 pipeline [44], and assigned taxonomy with the SILVA (v138) training set [45]. Sequencing read counts are available in Supplementary Data 1Z. Samples and sequence variants (SVs) were pruned such that the final dataset utilized in downstream taxonomic analyses retained samples with > 1000 reads, SVs present at > 1% relative abundance in any sample, and SVs with > 10,000 total reads across all urinary samples. Due to the low-abundance nature of the samples, additional stringent assessment using the decontam R package [46] was performed to assess the presence of likely contaminant SVs, after which one additional SV was removed from the dataset. Inferencing of microbial metagenomes was performed with PICRUSt2 [47, 48].

Whole shotgun metagenomic sequencing of stool samples

Fecal samples from 25 healthy control participants and 36 confirmed CaOx stone forming patients underwent shotgun metagenomic sequencing at The Centre for Applied Genomics at The Hospital for Sick Children in Toronto, ON, CAN. The SF samples were selected based on patients that had stone fragments extracted during surgery which were confirmed to be predominantly CaOx by Fourier transform infrared spectrophotometry. Samples from both cohorts were further pared to include only those surpassing DNA yield and quality thresholds: of the total 30 HC, 5 were excluded, and of the total 40 CaOx SF samples, 4 were excluded. DNA concentration was quantified using the Qubit™ dsDNA HS Assay Kit. Approximately 100 ng of DNA was PCR amplified and prepared for sequencing using the Nextera DNA Flex Library Prep Kit. The amplified library was purified and enriched for amplicons ~ 350 bp, then sequenced using an S1 Flowcell on the Illumina NovaSeq 6000.

Reads were exported as fastq files (BioProject ID PRJNA649273), quality assessed using FastQC [49], trimmed with Trimmomatic [50], and mapped against the human genome (Hg38) using Bowtie2 [51]. Sequencing read counts are available in Supplementary Data 1Z. Human reads were discarded, and the remaining unmapped reads were utilized in downstream analyses. The MGnify pipeline was used to annotate metagenomic functional potential [52]. Metagenomic bins were generated by mapping the reads from all samples to each raw assembly. MetaBat2 [53] was used to group contigs in the resultant alignment files based on their coverage and GC content. This process was repeated for sample-by-sample assemblies rather than a pooled assembly. Afterwards, all high-quality bins (assessed with CheckM [54]) were pooled together and dereplicated at 99% sequence identity using dRep [55]. Reads were then mapped back to the dereplicated set of genomes. PhyloPhlAn [56] was used to assign taxonomy to the bins, and counts were determined with Bowtie2. Taxonomic annotation was also performed with MetaPhlAn [57], which corroborated the PhyloPhlAn findings, but are not reported here. Functional annotation was also performed with the HUMAnN 3.0 pipeline [57], which generally corroborated the MGnify findings, but are not reported here.

High-performance liquid chromatography

Urinary oxalate concentration was measured in parts per million with HPLC and normalized to creatinine [58–60]. Reserved whole urine samples were thawed and vortexed for 30 s. Using PCR-grade filter tips, 50 μL of urine was transferred to an Eppendorf tube for creatinine quantification, and 950 μL of urine was transferred to a 15-mL conical tube for oxalate quantification.

For quantifying creatinine, 450 μL HPLC H_2O and 500 μL of HPLC acetonitrile were added to the urine and vortexed. The urine mixture was incubated at 4 °C for 15 min, facilitating precipitation of debris. Samples were then centrifuged for 15 min at 16,000 × *g* at 4 °C and filtered through 0.2-μm syringe filters into labelled amber HPLC vials (Agilent, Mississauga, ON, CAN). Standards of creatinine were prepared in HPLC H_2O at concentrations of 1, 5, 10, 50, 100, 150, 200, 250, and 300 ppm. The Agilent 1100 HPLC was utilized with the conditions stated in Supplementary Table 3.

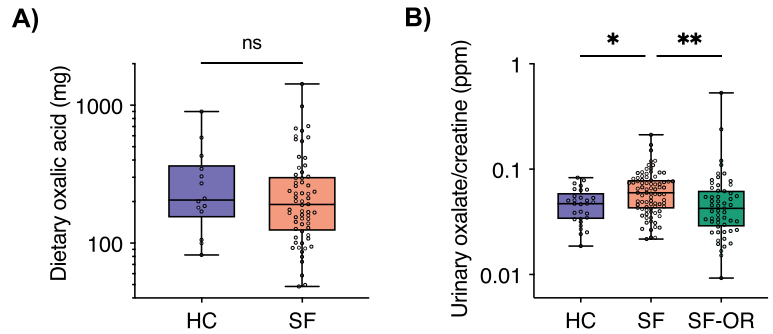

Fig. 1 Urinary, but not dietary oxalate levels differ between healthy controls and stone formers. **A** The approximate daily value of oxalic acid as measured through a diet history questionnaire was comparable between patient groups. HC ($n=14$), SF ($n=64$). **B** Urinary oxalate concentrations were determined with HPLC and normalized to creatinine levels. SF pre-operative urine had the highest oxalate concentrations (Kruskall-Wallis test with Dunn's multiple comparisons). Data represent the median (line in box), IQR (box), and minimum/maximum (whiskers); HC ($n=29$), SF ($n=83$), SF-OR ($n=55$)

For oxalate quantification, the 950 µL of urine (or oxalic acid standards at concentrations of 1, 10, 25, 50, 100, 150, 200, 250 ppm) was combined with 50 µL of 10 M HCl and 1 mL of 0.1 M *o*-phenylenediamine dissolved in 4 M HCl and vortexed. The tubes were capped, being careful to tighten the lids as much as possible. The tubes were then incubated in a laboratory oven at 100 °C for 6–7 h, then moved to 4 °C overnight. The following day, volume in the tube was carefully inspected and tubes that had experienced cracking or evaporation were discarded, requiring repeat processing. Five hundred microlitres of 200 mM $KHPO_4$ (pH 7.0) and 480 µL of 10 M KOH were added to the tubes with gentle vortexing. One millilitre of the mix was then transferred to labelled Eppendorf tubes and incubated at 4 °C for 15 min, then centrifuged for 15 min at 16,000 × *g* at 4 °C. Large pellets were present and were carefully avoided when transferring the entire volume to a 0.2-µm syringe filter; samples were filtered into labelled amber HPLC vials. The HPLC was utilized with the conditions stated in Supplementary Table 3.

Statistical analysis

Sequencing data analysis was performed conservatively in agreement with best practices in the field [61], using CoDaSeq, zCompositions, ALDEx2, ANCOM2, Vegan, and core R packages [62–71]. Specifically, significant confounders were determined with the envfit function from the Vegan R package [64] and accounted for in multivariate analysis with generalized linear models (GLM) using ALDEx2 (Supplementary Data) [62]. Fixed effect formulae used for GLM comparisons are reported in the Supplementary Data. All reported *P* values are corrected for false discovery rate (FDR) where applicable. In the microbiota differential abundance tests, significance was considered for FDR-corrected *P* values $P<0.1$ and/or effect size $>|0.5|$. For all other comparisons, $P<0.05$ was considered significant. The phylogenetic tree of shotgun metagenomic bin taxonomic annotations was generated with PhyloPhlAn [56] and visualized with iTOL [72]. The selection of balances for microbial signatures (R package selbal) was used to determine significant microbial signatures predictive of kidney stone disease [73]. Co-occurrence network analyses were performed with the R package NetCoMi [74]. Per-cohort network inference was performed on 1000 bootstrap iterations of Pearson correlation coefficients from CLR-transformed taxonomic and functional pathway count tables. Sample numbers, statistical significance, and names of statistical tests with corresponding FDR

(See figure on next page.)

Fig. 2 Compositional analysis of urine and stone microbiota. **A** PCA was performed on CLR-transformed Aitchison distances of all urine and stone samples. Each coloured point represents a sample. Distance between samples on the plot represents differences in microbial community composition, with 17.6% of total variance being explained by the first two components shown. Strength and association for genera are depicted by the length and direction of the grey arrows, respectively. Points are coloured by sample type and ellipses represent the 95% confidence intervals of sample types. Samples significantly differed by type and time (envfit *P* value <0.05). **B** Shannon's Index of alpha diversity was compared between sample groups. OR urine samples from stone patients had the lowest diversity (Kruskall-Wallis test with Dunn's multiple comparisons, * $P<0.05$, ** $P<0.01$, *** $P<0.001$). Data represent the median (line in box), IQR (box), and minimum/maximum (whiskers). **C** SVs were significantly distinct between stone former pre-operative urine compared to healthy control urine, stone former OR urine, and stones (Benjamini–Hochberg corrected Wilcoxon test $P<0.05$, ANCOM W value >0.7 threshold, ALDEx2 GLM effect size $>|0.5|$). Data represent the median and IQR; HC ($n=25$), SF ($n=83$), SF-OR ($n=59$), Stone ($n=34$)

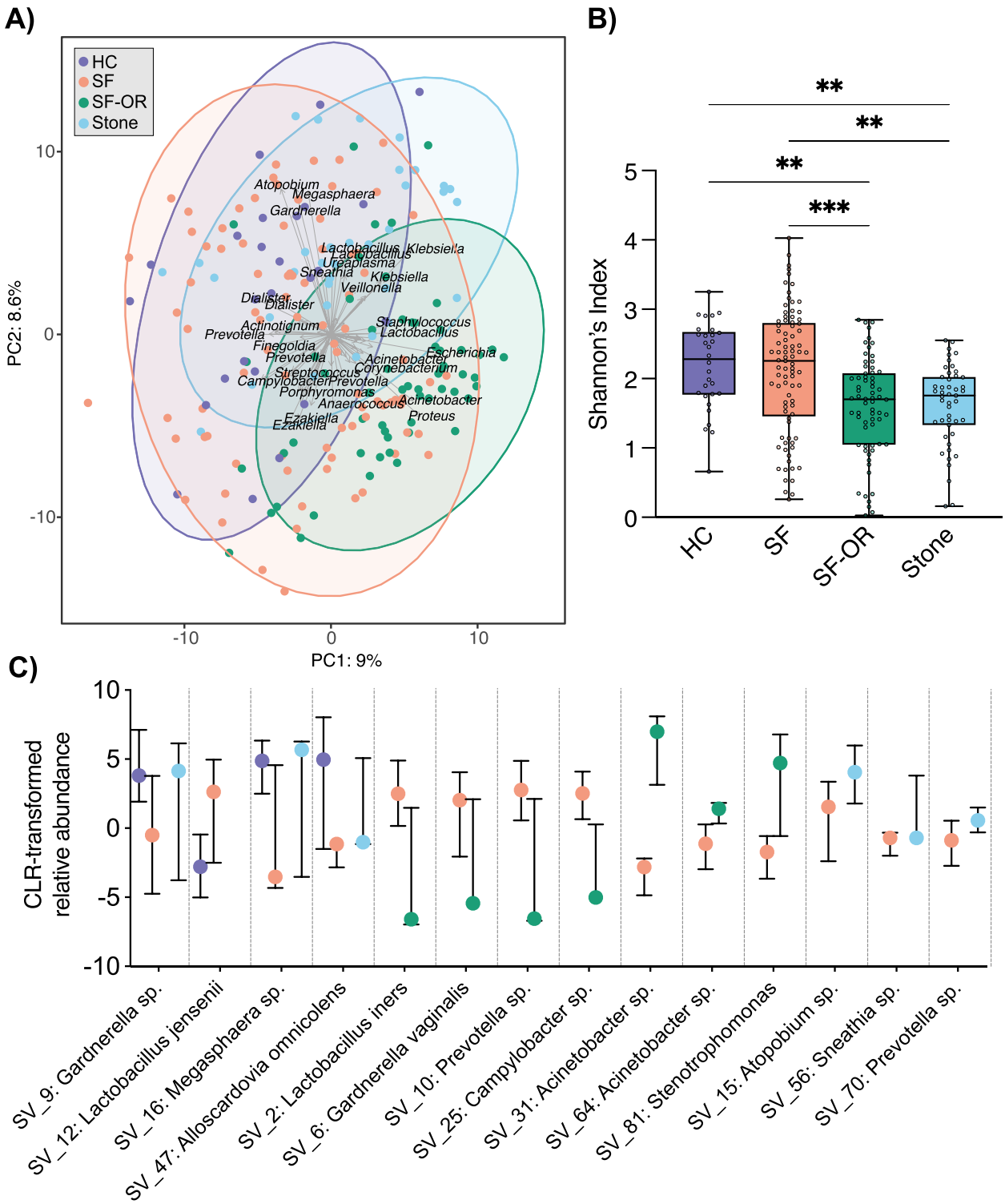

Fig. 2 (See legend on previous page.)

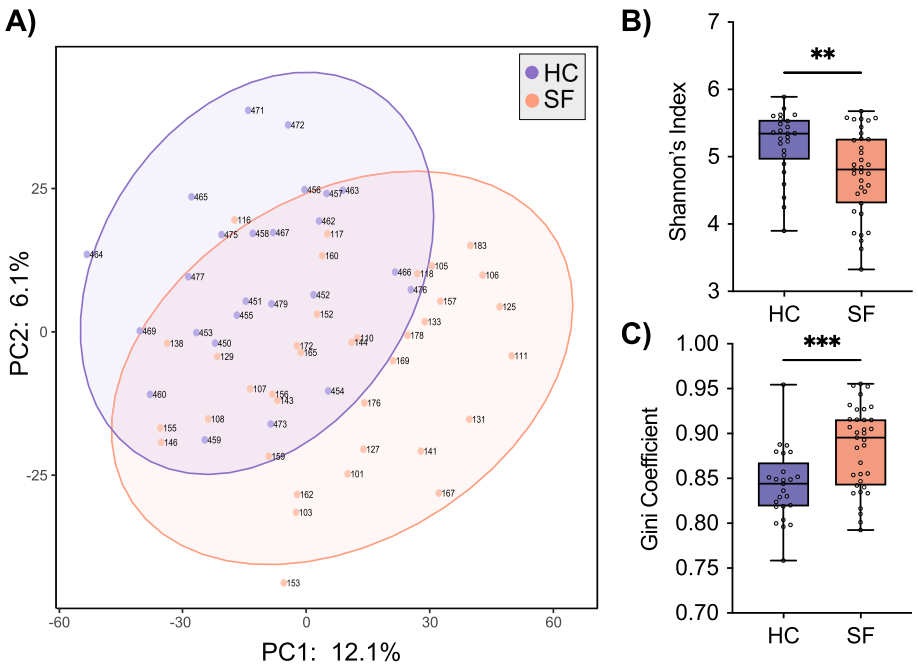

Fig. 3 Stone-former gut microbiota differs from healthy controls. **A** PCA was performed on CLR-transformed Aitchison distances of metagenomic taxonomic bin assemblies from HC and SF fecal samples. Each coloured point represents a sample. Distance between samples on the plot represents differences in microbial community composition, with 18.2% of total variance being explained by the first two components shown. Points are coloured by sample type and ellipses represent the 95% confidence intervals of sample types. Samples significantly differed by cohort (envfit *P* value < 0.1). **B** Shannon's Index of alpha diversity was significantly decreased in SF. **C** Gini coefficient of community inequality was significantly elevated in SF. Mann–Whitney tests, **P* < 0.05, ****P* < 0.001. Data represent the median, IQR, and minimum/maximum; HC (*n* = 25), SF (*n* = 36)

corrections are provided in the main text and figure legends for Figs. 1, 2, 3, 4, 5 and 6, Supplementary Figs. 1–4, and the Supplementary Data. Shapiro–Wilk tests of normality and statistical tests on participant metadata and urinary oxalate were performed in GraphPad Prism (v8.3.1) and R.

Results

Kidney stone microbiome (KiSMi) cohort characteristics

The KiSMi cohort consisted of 113 participants, of which 83 were SF and 30 were HC (Supplementary Data 1A). This yielded 179 urine samples, 113 oral swabs, 47 stone fragments, and 102 fecal samples (Supplementary Fig. 1). HC were matched to SF based on age, sex, and most comorbidities (Supplementary Data), but differed in their history of UTI, smoking status, and antibiotic history. However, no participants had antibiotic exposure for at least 90 days prior to enrollment and initial sample collection (SF had prophylactic antibiotic exposure at the OR timepoint) (Table 1). SF were evenly divided between those who received percutaneous nephrolithotomy (PCNL) compared to ureteroscopic (URS) surgery. Of SF, 84% had recurrent kidney stones and 77% were CaOx stone formers. HC and SF participants did not significantly differ in their estimated dietary intake of oxalate (Fig. 1A), nor any of the other 216 measured features from the diet history questionnaire after correcting for false discovery rate; however,

(See figure on next page.)

Fig. 4 Phylogeny and differentially abundant gut microbiota taxa. **A** A maximum-likelihood phylogenetic tree of dereplicated genomes from the gut microbiota. The outermost grey bars represent the overall prevalence of the taxonomic bin. Orange and purple dots in the second layer denote taxonomic bins that were significantly more abundant in SF or HC, respectively (Benjamini–Hochberg corrected Wilcoxon test (*P* < 0.1) and effect size > |0.5|). Tree branches are coloured by phylum. **B** Average relative phylum abundance bar plot of HC and SF cohorts. Each vertical bar represents the average relative abundance within the cohort, coloured by phylum. **C** Effect sizes of taxa are coloured by cohort of enrichment and labelled where taxonomic information is available. Coloured species were significantly different by Benjamini–Hochberg corrected Wilcoxon test (*P* < 0.1) and effect size > |0.5|

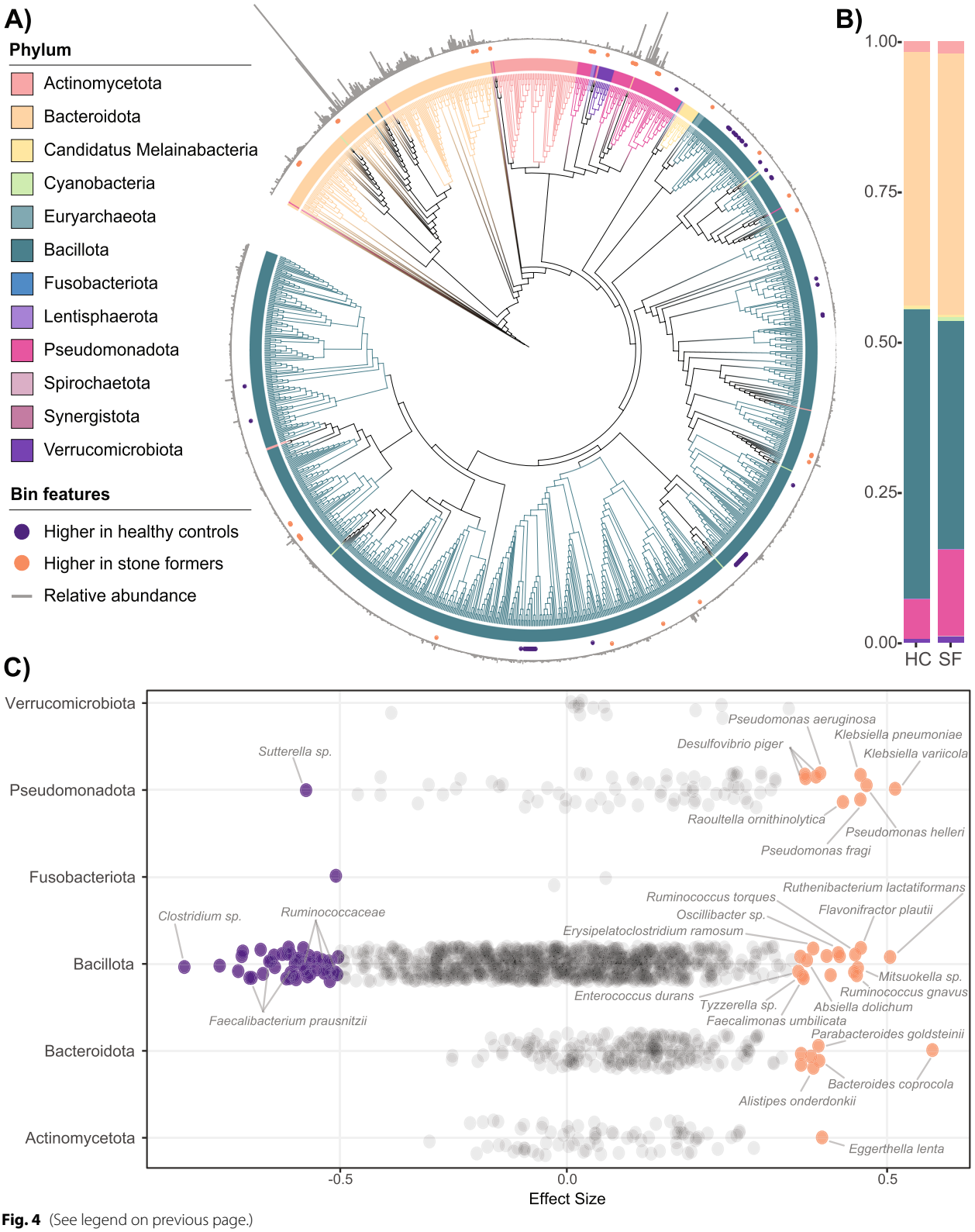

Fig. 4 (See legend on previous page.)

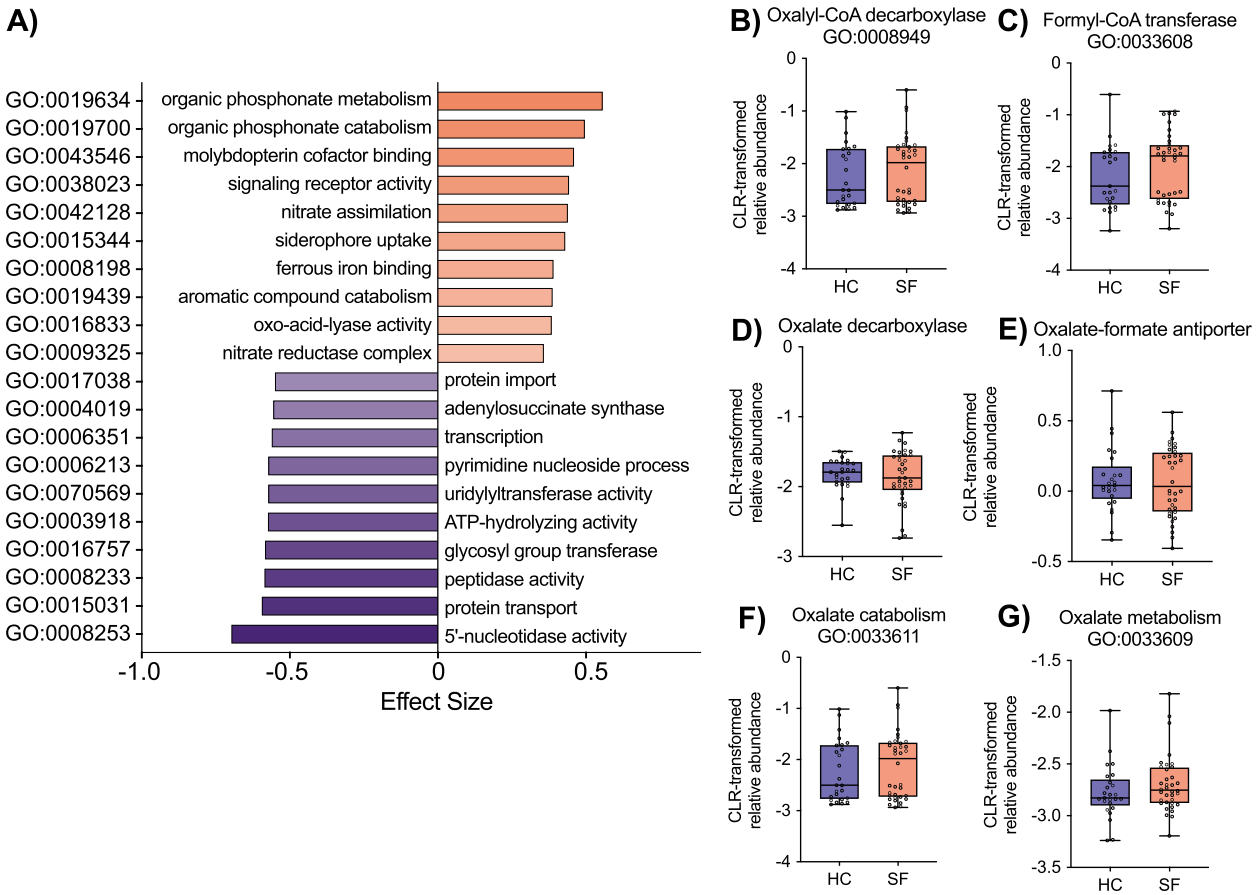

Fig. 5 SF gut microbiota differs functionally from HC, but not in direct oxalate handling. **A** Effect size of the ten most differentially abundant gene ontology (GO) terms per cohort are coloured by cohort of enrichment. All GO terms shown were significantly different by Benjamini–Hochberg corrected Wilcoxon test ($P < 0.1$). **B–G** The relative abundance of oxalate handling genes was not different between cohorts by Bonferroni corrected Mann–Whitney *U* test. Data represent the median, IQR, and minimum/maximum; HC ($n = 25$), SF ($n = 35$)

several trends were observed in decreased vitamin, saturated fatty acid, phytoestrogen, and other micronutrient levels (Supplementary Fig. 2, Supplementary Data 1B, C). The urinary oxalate/creatinine ratio was significantly higher in the SF patients at the pre-operative time point compared to HC and SF at the OR timepoint (Fig. 1B, Supplementary Data 1D).

16S rRNA gene amplicon sequencing reveals distinct multi-site taxonomic and functional communities in SF

The most proportionally abundant genera in the urinary and stone dataset were *Escherichia* (29.7%), *Lactobacillus* (12.8%), *Staphylococcus* (10.3%), *Gardnerella* (7.3%), and *Streptococcus* (7.3%) (Supplementary Data 1E). The sequence counts were centred log ratio (CLR) transformed and a Euclidian distance was applied, generating sample-wise Aitchison distances, which were analysed with principal components analysis (PCA) [68]. The PCA biplot displays clustering of samples based on sample type, which was validated by *envfit* from the R package vegan ($P < 0.05$) (Fig. 2A, Supplementary Data 1F). Sample types differed by alpha diversity, whereby SF urine collected during stone removal surgery (OR urine) had the lowest Shannon's index, and the HC and pre-operative SF urine samples had the highest (Fig. 2B, see Supplementary Data 1G-H for additional alpha diversity metrics). As sample type (stone vs. urine) and time (pre-operative vs. OR) were deemed significant drivers of microbiota variation (*envfit* $P < 0.05$), samples were investigated in separate comparisons on these bases to determine significantly altered taxa while adjusting for significant covariates (Supplementary Data 1F). The relative abundance of several SVs was discordant between the urine from HC and SF, SF and SF-OR, and SF urine and stones (Benjamini–Hochberg corrected Wilcoxon test with ALDEx2, and ALDEx2 GLMs; Fig. 2C, Supplementary Data 1I). Specifically, *Gardnerella* sp., *Megasphaera* sp., and *Alloscardovia omnicolens* were relatively more abundant in HC urine compared to SF urine, whereas *Lactobacillus jensenii* was relatively enriched in SF.

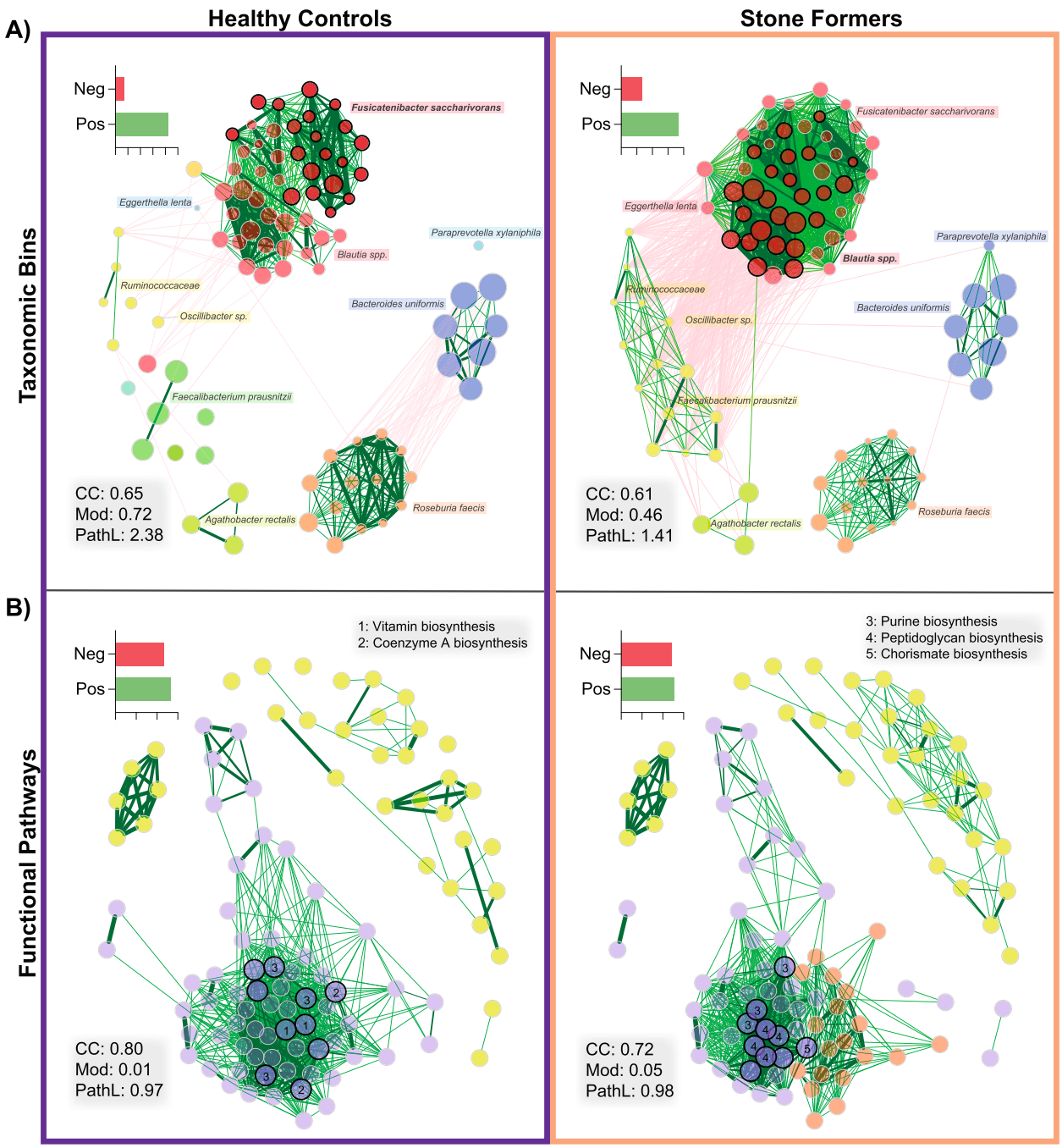

Fig. 6 Co-occurrence networks demonstrate divergent community structures between HC and SF. Network inference was built upon 1000 bootstrap iterations of Pearson correlation coefficients from CLR-transformed taxonomic and functional pathway counts. **A** Nodes represent individual taxonomic bins, and clusters are labelled with corresponding species; the fifty nodes with the highest degree are displayed. **B** Nodes represent functional pathways; the eighty nodes with the highest degree are displayed. Nodes are coloured by clusters and sized by their CLR-transformed abundance, with nodes in bold representing hubs. Numbers within hubs correspond to the common functional pathways of interest. Edges with positive estimated interactions are coloured in green, and negative estimated interactions are coloured in red; percentage of edge positivity is displayed in the inset bar chart. CC = clustering coefficient, Mod = modularity, PathL = average path length

Within stone patients, *Lactobacillus iners*, *G. vaginalis*, *Prevotella* sp., and *Campylobacter* sp. were relatively depleted at the OR timepoint (following antibiotic exposure and collected via catheter), while the nosocomial pathogens *Acinetobacter* spp. and *Stenotrophomonas* sp. were enriched. Compared to SF urine samples, stones harboured relatively more *Gardnerella* sp., *Megasphaera* sp., *A. omnicolens*, *Atopobium* sp., *Sneathia* sp., and

Table 1 KiSMi study participants characteristics

Metric		Healthy controls	Stone patients	*P* value
No. enrolled		30	83	
Sex		**n (%)**	**n (%)**	
	Female	11 (37)	32 (39)	
	Male	19 (63)	51 (61)	0.99[a]
Age		**M (SD)**	**M (SD)**	
		55 (11.1)	58 (11.5)	0.28[b]
BMI		**M (SD)**	**M (SD)**	
		27.6 (4.6)	30.2 (7.0)	0.08[c]
Other health features		**n (%)**	**n (%)**	
History of stones		0 (0)	70 (84)	<0.0001[a]
History of UTI		9 (30)	43 (52)	0.05[a]
Smoking status				
	Current smoker	0 (0)	12 (14)	
	Non-smoker	30 (100)	71 (86)	0.03[a]
Comorbidities	**Cardiac**	3 (10)	8 (10)	0.99[a]
	Hypertension	8 (27)	32 (39)	0.37[a]
	Diabetes	3 (10)	12 (14)	0.75[a]
	Hypothyroidism	3 (10)	9 (11)	0.99[a]
Years since antibiotic use		**M (SD)**	**M (SD)**	
		5.53 (5.8)	3.4 (4.0)	0.004[c]
Stone removal procedure			**n (%)**	
	PCNL		40 (48)	
	Ureteroscopy		43 (52)	
Major stone component				
	Calcium oxalate		40 (77)	
	Calcium phosphate		1 (2)	
	Uric acid		7 (13)	
	Struvite		3 (6)	
	Cystine		1(2)	
	Unknown (not tested)		31	

[a] Fisher's exact test of categorical variables

[b] Unpaired two-tailed t-test for normally distributed continuous variables

[c] Mann-Whitney U test for non-normally distributed continuous variables

Prevotella sp. Stones of calcium, struvite, uric acid, and cystine compositions harboured a microbiota surpassing the stringent filtering conditions implemented; however, potentially due to small sample sizes when sub-grouped by stone type, the microbiota was not driven by crystalline composition (*envfit* $P > 0.05$, Supplementary Data 1F and Supplementary Fig. 3).

Functional inferencing of the urinary samples revealed numerous genetic functions and pathways that were enriched in SF (pre-operative) relative to HC (Supplementary Data 1 J-K), including virulence-associated iron acquisition [75], enterobacterial common antigen biosynthesis [76], polmyxin resistance [77], stress-response ppGpp biosynthesis [78], and most significantly (standardized effect size 0.78) pyridoxine (vitamin B6) biosynthesis. Vitamin B6 is a cofactor for over 140 reactions in humans [79], including the detoxification of glyoxylate to glycine by the enzyme alanine-glyoxylate aminotransferase (AGT); deficiency of this vitamin and subsequent reduction in AGT activity can lead to increased urinary oxalate excretion [80, 81]. Thus, while systemic and intestinal vitamin B6 may have therapeutic benefits for stone formers, its role in the bladder is not well understood, and conversely has been anecdotally attributed to bladder sensitivity and incontinence symptoms [82, 83]. In contrast, urinary samples from SF were significantly depleted relative to HC in vitamin B12 biosynthesis, butyrate

biosynthesis, and several basal bioenergetic enzymatic pathways.

The salivary microbiota from both cohorts was dominated by *Streptococcus* spp. (average abundance > 50%), followed by *Haemophilus*, *Gemella*, and *Escherichia* spp. (3–5%) (Supplementary Data 1L). While saliva samples from SF trended towards an increased relative abundance of the periodontal pathobionts *Porphyromonas endodontalis*, *Fusobacterium nucleatum*, and *Prevotella* sp., alongside depleted *Streptococcus* spp. compared to HC, this did not reach statistical significance after multiple testing correction and adjusting for significant covariates (Supplementary Data 1M), nor did differences based on functional inference testing (Supplementary Fig. 4, Supplementary Data 1N-P). However, the saliva samples from SF had significantly higher diversity than HC by multiple diversity metrics (Supplementary Data 1Q-R).

Shotgun metagenomic sequencing reveals significant alterations in SF gut microbiota

A total of 102 fecal samples were collected from which DNA was extracted. Of these, 61 were selected for deep profiling with whole shotgun metagenomic sequencing. These comprised samples from 25 HC, and 36 confirmed CaOx SF, all with adequate DNA yield and quality for shotgun library preparation. Sample 153 was deemed to be an outlier via the CoDaSeq R package [67] and removed from downstream analyses (Fig. 3A). Samples separated by cohort based on PCA (Fig. 3A), and alpha diversity metrics (Fig. 3B, C). Specifically, Shannon's index was significantly decreased in SF, and Gini coefficient of community inequality was significantly increased, illustrating that the SF harbour a gut microbiota with less diversity and more unequal distribution of taxa (Supplementary Data 1S-T).

Corroborating previous studies, *Faecalibacterium prausnitzii*, *Agathobacter rectalis*, *Bacteroide*s spp., *Roseburia* spp., *Alistipes* spp., *Ruminococcus* spp., and *Blautia* spp. were among the highest relative abundances across all gut samples (Fig. 4A, Supplementary Data 1U) [84, 85]. After correcting for significant covariates (Supplementary Data 1V), eighty-two bacterial taxa were differentially abundant between HC and SF, including relative enrichment of numerous pathobionts and disease-associated microbes in SF, with notable decreases in unclassified taxa from the phylum Bacillota and the health-associated *F. prausnitzii* (Fig. 4B, Supplementary Data 1W). *O. formigenes* abundance was not differentially abundant between cohorts, and similar to recent reports was only detected at very low abundance in two SF participants [21]. There were no significant differences between HC and SF in archaeal or eukaryotic taxa; however, a *Faecalibacterium* phage virus (*Taranisvirus*) was enriched in HC (effect size 0.53, Supplementary Data 1W).

The selection of balances (selbal) [73] was utilized to identify microbial signatures most predictive of stone disease. At the taxa level, the balance most associated with SF status was resolved through higher relative abundance of *Desulfovibrio piger* with respect to *Clostridium* sp. AM49-4BH and an unknown taxon from the phylum Bacillota (Supplementary Fig. 5A). At the genus level, the balance most associated with SF status was resolved through a higher relative abundance of *Pseudomonas* and *Proteus* with respect to an unknown genus from the phylum Fusobacteriota (Supplementary Fig. 5B).

Functionally, SF were significantly depleted in the relative abundance of numerous essential housekeeping functions (protein transport, transcription, bioenergetic machinery) and enriched in virulence and inflammatory processes (phosphonate metabolism [86], molybdopterin enzymatic processes [87], nitrate utilization [88], and iron acquisition [75]) (Fig. 5A, Supplementary Data 1X). In contrast, no differences were observed between cohorts in any of the genes associated with direct oxalate handling investigated here (Fig. 5B–G). Interestingly, bacterial uridylyltransferase activity was depleted in SF (Supplementary Data 1X), an enzyme that when deficient in humans can result in CaOx kidney stone formation via galactosemia [89].

Network analysis reveals community-wide imbalance in SF microbiota

Co-occurrence networks were constructed for taxonomic and functional profiles of the gut microbiota to determine significant interactions (Fig. 6A, B). Both qualitatively and quantitatively, the taxa network was strikingly different between HC and SF cohorts (Fig. 6A, Supplementary Data 1Y), with significantly different network hubs ($P = 0.028$, all *Fusicatenibacter saccharivorans* in HC, and the majority *Blautia* spp. in SF), correlations, and overall structure (betweenness centrality $P < 0.0001$). Of note, the network hubs in SF were strongly negatively correlated with core health-associated gut microbes such as *F. prausnitzii* [90], and positively correlated with the inflammation-associated and SF-enriched *E. lenta* [91], while those correlation patterns were absent in HC. Network modularity, a marker of evolutionarily well-adapted community function [92], was also lower in SF (0.72 in HC vs. 0.46 in SF).

The network of interactions modelled on functional pathways also contrasted between cohorts (Fig. 6B), with significantly different network hubs ($P = 0.032$) and overall structure (betweenness centrality $P < 0.0001$). Hubs of folate, riboflavin, and coenzyme A biosynthesis were absent in SF, while peptidoglycan biosynthesis, and

potentially virulence-associated hubs including purine [93, 94] and chorismate biosynthesis [95], were present. Of note, the overarching hub cluster with connection to major housekeeping functions such as glycolysis and coenzyme A biosynthesis was severed in SF. These network findings demonstrate that rather than a single or set of few microbes driving differences between the cohorts, there is a complete divergence of SF microbiome structure at a systems-level compared to HC.

Discussion

This study demonstrated that independent of diet, the microbiome in stone formers is altered at multiple anatomical sites — evidence of a systemically diseased population and a role for the microbiome beyond direct oxalate handling in CaOx kidney stone formation. Notably, we identified reduced diversity, altered taxonomic structure, and functional bioenergetic collapse coupled with an enrichment of virulence-associated gene markers in both the urinary and gut microbiota. Markers of health such as vitamin production, butyrate biosynthesis, and core beneficial taxa were comparatively displaced by virulence factors, antimicrobial resistance elements, and pathobionts, in both the urinary and gut microbiota of SF. These multi-site microbial community shifts may be the result of deleterious environmental factors including antibiotic exposure. Based on these findings, we suggest that the historic emphasis put on *O. formigenes* and other direct oxalate-handling taxa should be discontinued in favour of mechanistic study into the apparent systems-level microbial imbalances in SF.

Previous studies investigating the bacterial contribution to this disease, even those employing whole shotgun metagenomic sequencing techniques, have limited their focus to intestinal bacteria that degrade oxalate and the corresponding direct oxalate-handling genes [13, 18, 21, 22, 96, 97]. Several more recent studies have evaluated the gut microbiota in stone disease and described generalized "dysbiosis" and reduced diversity, but a consensus on the specific alterations has not been obtained [16, 17, 22–26]. Moreover, studies into the urinary and stone microbiota of stone formers have been prefatory, involving few patients or lacking an appropriately matched healthy control comparison group [16, 29–32]. Despite lacking a consensus on specific findings, as a collective this previous work has robustly indicated that the microbiome in stone formers significantly differs from a healthy state [98].

It is estimated that 20–50% of urinary oxalate results from dietary consumption [99]. In concordance with previous studies, it was confirmed here that stone patients had higher urinary oxalate concentrations (Fig. 1B) despite comparable measures of dietary oxalate consumption as measured by diet history questionnaire (Fig. 1A) [100]. The urinary microbiota was significantly distinct between HC and SF, and in SF throughout their course of treatment. Specifically, at the time of surgery SF were enriched in inflammatory, antibiotic-resistant, nosocomial infection-associated microbes and their accompanying virulence factors (*Acinetobacter* [101] and *Stenotrophomonas* spp [102]) and compositionally depleted in typically benign members of the urinary microbiota (*Lactobacillus*, *Gardnerella*, and *Prevotella* spp., Fig. 3C) [103]. However, the OR urine samples were collected via catheter (in comparison to the pre-operative samples which were clean-catch), which in addition to the concurrent antibiotic exposure may bias these results. Although further research is needed to conclusively determine the cause, it is possible that relative depletion of the normal urinary microbiota with pre-surgical antibiotic treatment may allow for antibiotic-resistant, deep-seated uropathogens to dominate the niche [104]. Efforts should be made to understand the permanence and clinical implications for such substantial adverse urinary microbiota changes occurring in the short time frame prior to stone surgery.

We confirmed the presence of a sequence-positive microbiota in all stone crystalline compositions, expanding upon previous work by others [16, 29–31, 105]. The stone microbiota was derived from urogenital microbes, yet compositionally distinct from both pre-operative and intraoperative urine (Fig. 2C), indicating that bacteria inside calculi likely do not derive out of coincidental entrapment in the growing stone matrix. Instead, the results suggest that specific microbes are intimately involved in stone development, potentially exacerbating crystal nidus formation through inflammation and crystal aggregation [15, 30, 106, 107]. By fragmenting the calculi, in combination with the often-accompanying antibiotic exposure, surgical stone intervention may be a seeding opportunity for antibiotic-resistant stone-bound bacteria, and perhaps could play a role in the extremely high recurrence rate following surgical stone treatment [108, 109].

The distant site of the oral cavity microbiota was investigated here due to its known associations with systemic diseases such as rheumatoid arthritis [110], cardiovascular disease [111, 112], and cancer [113, 114]. Although not reaching statistical significance with multiple testing corrections, the trends in the current study of increased relative abundance of pathobionts such as *F. nucleatum*, *P. endodontalis*, and *Prevotella* spp. in SF relative to HC further points to a systemically diseased population, rather than the loss of a single gut microbe or function (oxalate degradation). With regard to microbiota analysis,

saliva samples are thought to represent the pool from several distinct sites in the oral cavity, so more targeted sampling such as within the periodontal pocket may yield a higher correlation with stone formation. These microbes can easily translocate into circulation through inflamed oral mucosa leading to systemic immune dysregulation [114] and they are also consumed in saliva, seeding the gut microbiota [115]. Thus, it is possible but yet unknown whether the oral microbiota could be acting as a biomarker of KSD or actively implicated in KSD progression; future work should investigate these mechanistic relationships in greater depth.

Longstanding dogma has held that intestinal colonization by *O. formigenes* lowers oxaluria and consequently the risk of stone formation; however, recent studies have failed to detect differences in the colonization rates between stone formers and non-formers [12, 18, 116–118]. In congruence with other recent studies [17, 19, 22], we did not detect a difference in the relative abundance of this bacterium in fecal samples from HC and calcium oxalate (CaOx) SF by whole shotgun metagenomic sequencing. Rather, we found that the gut microbiota significantly differed between cohorts based on alpha diversity, relative taxonomic composition, functional potential, and overall network structure. These alterations are still likely implicated in CaOx nephrolithiasis; however, a clear oxalate-degrading role is not apparent based on these data.

F. prausnitzii is a beneficial, butyrate-producing core gut commensal and was found in the current Canadian KiSMi cohort to be significantly depleted in SF in terms of taxonomic abundance as well as through attributed function and viral phage [90, 119]. These findings echo preliminary work by Ticinesi et al. [18] and Liu et al. [26], who performed shotgun metagenomic sequencing on a small number of their Italian and Chinese patients (both $N=5$ per cohort), as well as Kim et al. [20] and Chen et al. [120] who performed 16S amplicon sequencing on larger Korean and Chinese cohorts, respectively, demonstrating the reproducibility of depleted *Faecalibacterium* in stone formers on a global scale. Although generally associated with health, depletion of this microbe may specifically be involved in nephrolithiasis through its crucial role as a butyrate producer [121]. Butyrate enhances tight junction assembly [122], preventing intestinal permeability and potentially decreasing passive paracellular oxalate uptake [123]. It may also have a role in active transcellular uptake mechanisms by modulating the expression of the oxalate transporter SLC26A6 [124], and even decreasing crystal formation in the kidney through immune modulation [125].

Other gut microbiota alterations detected here have potential implications for nephrolithiasis in SF, including the enrichment of *Desulfovibrio* spp. (a significant signature of SF by *selbal* analysis) and *Flavonifractor plautii*. The intestinal oxalate-sulfate antiporter (SAT-1) has been implicated in human CaOx nephrolithiasis [126]; as sulfate-reducing bacteria, *Desulfovibrio* spp. may reduce the bioavailability of the influx substrate leading to greater plasma oxalate levels, as is observed in cohorts with Autism [127, 128]. *F. plautii* is a flavonoid-degrading bacterium, but dietary plant flavonoids have been shown to be beneficial in stone and cancer cohorts [129], potentially reducing the incidence of CaOx stones through diuretic, anti-oxidant, and anti-inflammatory mechanisms [130]. More broadly, *Eggerthella*, *Flavonifractor*, and *Ruminococcus* spp., all of which were enriched in SF, have recently been suggested as general disease-associated signatures (shared across type 2 diabetes, diarrhoea and constipation, mental disorders, and gallstones) in a cohort of over 8000 extensively characterized Dutch individuals [90]. Additionally, the SF gut was enriched in a variety of uropathogenic Gammaproteobacteria including *Pseudomonas* spp. and *Proteus* spp. (significant signatures of SF by *selbal* analysis) as well as *Klebsiella* spp.. The gut is a known reservoir for uropathogens [131], thus the relevance of these organisms' enrichment in SF goes beyond intestinal colonization as these bacteria have themselves been cultured from calcium-based stones, and may be exacerbating formation [31, 106]. The balance analysis indicating *Desulfovibrio piger*, *Proteus*, and *Pseudomonas* spp. as significant signatures of SF relative to unclassified taxa from the phyla Bacillota and Fusobacteriota requires further confirmatory study, but these taxa hold promise as potential future biomarkers of stone disease diagnosis or pathogenesis.

Previous literature demonstrates that antibiotic exposure is associated with stone formation [21, 132]. In congruence, our findings that SF had significantly more recent antibiotic use, and the enrichment in antibiotic resistance genes and taxa support the notion that antibiotic exposure (from childhood up to and during stone treatment) corrupts both the urinary and gut microbiota leading to inflammation, loss of beneficial function, and a bloom of uropathogens which may be exacerbating stone formation [133].

Although this work has demonstrated a critical association of the microbiota in kidney stone disease, limitations of the current study must be considered. These data were derived from a single centre from a relatively ethnically homogenous patient population, and thus should be replicated in an independent and ethnically diverse cohort. Several patient factors including smoking status, UTI, and antibiotic exposure history were discordant between

the current cohorts, so a future study with larger matched sample sizes would increase the precision of the current findings (particularly the predicted biomarker taxa). No differences were determined between the HC and SF cohorts based on diet as measured by the validated food frequency questionnaire; however, results from this questionnaire may be biased through self-reporting and yearly estimation. Future studies could employ a standardized diet or detailed food diary to more accurately estimate the dietary micro- and macronutrients directly prior to sample collection. In a similar manner, the participants' antibiotic exposure history was self-reported, which is also subject to bias. In future studies where the healthcare infrastructure permits, a more detailed medical record of antibiotic exposures should be utilized.

This study employed 16S rRNA amplicon sequencing of the urinary and saliva samples, and whole shotgun metagenomic sequencing of the stool samples; these techniques provide relative compositional, but not absolute abundance information. Both sequencing methods did not provide taxonomic annotation to the species level in all cases. For this reason, as well as the problematic nature of comparing across sequencing methodologies, caution should be taken when comparing these data and taxonomic annotations in future studies. Further, future research could employ genomic assemblies from the shotgun dataset to explore species-specific taxonomy. The 16S rRNA amplicon data were used to infer functional metagenomes with PICRUSt2; although this technique demonstrates accuracy in samples of human origin, it is based on variation in the amplicon region to predict the entire genome, and thus is unable to differentiate strain-level functionality [47, 48]. This technique is not a replacement for whole shotgun metagenomic sequencing, which could be employed in the future to validate the current findings. Although fecal samples were collected in accordance with a previously validated protocol, they were collected on toilet paper and may have been exposed to skin-derived or environmental microbes. HC and initial SF urine samples were collected as clean-catch midstream samples; however, this may not capture bacteria adhered to the uroepithelium. Rather than the clean-catch method, SF-OR samples were collected during surgery via catheter, which likely accounts for some of the differences between the SF urine samples over time; in the future, HC and initial SF urine samples could also be collected via catheter for additional comparability. Although a multivariate analysis was undertaken, a future study in a larger sample size could have better precision in detecting and adjusting for potential confounders due to patient comorbidities and lifestyle factors. Finally, this was an observational study, thus we cannot attribute causality of stone disease to the differences detected between the microbiota of HC and SF.

Conclusions

Together, the SF-associated markers detected in this study are indicative of a systemically diseased population and may hold greater explanatory power regarding nephrolithiasis risk than direct oxalate degradation or *O. formigenes* presence. We propose that a more inconspicuous method of oxalate homeostasis is likely causative and dependent on an evolutionarily adapted gut microbiota. If the diversity and robust functional potential of the healthy human microbiome is repeatedly assaulted by the average Westernized lifestyle via antibiotic exposure, diet, and other environmental factors, kidney stone prevalence will continue to increase. To prevent the cyclic recurrence of this disease, future management of nephrolithiasis should incorporate both the prevention of microbiome disturbance and the use of agents for subsequent restoration of homeostasis.

Abbreviations

BMI	Body mass index
CaOx	Calcium oxalate
CLR	Centred log ratio
FDR	False discovery rate
GLM	Generalized linear model
HC	Healthy controls
HPLC	High-performance liquid chromatography
IBD	Inflammatory bowel disease
KSD	Kidney stone disease
OR	Operating room
PCA	Principal component analysis
PSNL	Percutaneous nephrolithotomy
SF	Stone formers
SV	Sequence variant
URS	Ureteroscopy
UTI	Urinary tract infection

Supplementary Information

The online version contains supplementary material available at https://doi.org/10.1186/s40168-023-01703-x.

Additional file 1. Supplementary Data.

Additional file 2: Supplementary Figure 1. KiSMi cohort sample collection. **Supplementary Figure 2.** Dietary macronutrients are comparable between cohorts. **Supplementary Figure 3.** Kidney stone microbiota is not dictated by stone composition. **Supplementary Figure 4.** Oral salivary microbiota is comparable between cohorts. **Supplementary Figure 5.** Gut microbiota global balances predictive of kidney stone disease. **Supplementary Table 1.** KiSMi study participant inclusion and exclusion criteria. **Supplementary Table 2. 1**6S rRNA primer and barcode sequences. **Supplementary Table 3.** HPLC running conditions.

Acknowledgements

We thank Linda Nott and Dr. Patricia Rosas-Arellano for logistical support and sample collection. We also thank Dr. Thomas Tailly, Dr. Daniel Olvera-Posada, and Dr. Abdulaziz Al-Athel for performing ultrasound exams on healthy control participants. We thank David Carter at London Regional Genomics

Centre and Dr. Sergio Pereira at The Centre for Applied Genomics for sample processing and sequencing. This work was supported by the W. Garfield Weston Foundation. We acknowledge the Anishinaabek, Haudenosaunee, Lūnaapéewak, and Chonnonton Nations, whose traditional territories are where this study was undertaken, and the publication was produced.

Author's Twitter handle

@Our_MicroBiome (Jeremy P. Burton)

Authors' contributions

Conceptualization, G.R., J.D.D., H.R., and J.P.B.; Methodology, K.F.A., B.R.J., B.A.D., J.A.C., J.B., G.B.G., and J.P.B.; Formal analysis, K.F.A., B.R.J., and B.A.D.; Investigation, K.F.A; Resources, G.B.G., J.D.D., H.R., and J.P.B.; Data curation, K.F.A., B.R.J., B.A.D., and G.B.G.; Writing—original draft, K.F.A.; Writing—review and editing, K.F.A., B.R.J., B.A.D., J.A.C., J.B., G.R., G.B.G, J.D.D, H.R., and J.P.B; Supervision, G.R., G.B.G., J.D.D., H.R., and J.P.B; Funding acquisition, J.P.B.

Funding

Funding for this study was generously provided by the W. Garfield Weston Foundation.

Availability of data and materials

The datasets supporting the conclusions of this article are available in the NCBI Sequence Read Archive: BioProject ID PRJNA856314 (urinary 16S dataset), and PRJNA856641 (oral 16S dataset), and PRJNA649273 (gut shotgun metagenomic dataset). Input counts, taxonomy annotation, and metadata tables are available at Zenodo (https://doi.org/10.5281/zenodo.7199455), and custom scripts are available at https://github.com/kait-al/KiSMi-Kidney-Stone-Microbiome. All other data generated or analysed during this study are included in this published article and its supplementary information files.

Declarations

Ethics approval and consent to participate

Ethical approval for the KiSMi study was granted by Lawson Health Research Institute (CRIC R 15–117) and the Health Sciences Research Ethics Board at the University of Western Ontario (REB #105443) in London, Ontario. Written consent was obtained from all the study participants at the time of study inclusion and the methods were carried out in accordance with the 1approved guidelines.

Consent for publication

Not applicable.

Competing interests

The authors declare that they have no competing interests.

Received: 30 November 2022 Accepted: 17 October 2023
Published online: 25 November 2023

References

1. Pearle MS, Calhoun EA, Curhan GC. Urologic Diseases of America P: Urologic diseases in America project: urolithiasis. J Urol. 2005;173:848–57.
2. Scales CD Jr, Curtis LH, Norris RD, Springhart WP, Sur RL, Schulman KA, Preminger GM. Changing gender prevalence of stone disease. J Urol. 2007;177:979–82.
3. Scales CD Jr, Smith AC, Hanley JM, Saigal CS. Urologic Diseases in America P: Prevalence of kidney stones in the United States. Eur Urol. 2012;62:160–5.
4. Tasian GE, Ross ME, Song L, Sas DJ, Keren R, Denburg MR, Chu DI, Copelovitch L, Saigal CS, Furth SL. Annual Incidence of Nephrolithiasis among Children and Adults in South Carolina from 1997 to 2012. Clin J Am Soc Nephrol. 2016;11:488–96.
5. Abufaraj M, Xu T, Cao C, Waldhoer T, Seitz C, D'Andrea D, Siyam A, Tarawneh R, Fajkovic H, Schernhammer E, et al. Prevalence and Trends in Kidney Stone Among Adults in the USA: Analyses of National Health and Nutrition Examination Survey 2007–2018 Data. Eur Urol Focus. 2021;7:1468–75.
6. Gan XT, Ettinger G, Huang CX, Burton JP, Haist JV, Rajapurohitam V, Sidaway JE, Martin G, Gloor GB, Swann JR, et al. Probiotic administration attenuates myocardial hypertrophy and heart failure after myocardial infarction in the rat. Circ Heart Fail. 2014;7:491–9.
7. Gurung M, Li Z, You H, Rodrigues R, Jump DB, Morgun A, Shulzhenko N. Role of gut microbiota in type 2 diabetes pathophysiology. EBioMedicine. 2020;51: 102590.
8. Turnbaugh PJ, Ley RE, Mahowald MA, Magrini V, Mardis ER, Gordon JI. An obesity-associated gut microbiome with increased capacity for energy harvest. Nature. 2006;444:1027–31.
9. Moe OW. Kidney stones: pathophysiology and medical management. Lancet. 2006;367:333–44.
10. Hatch M, Freel RW. The roles and mechanisms of intestinal oxalate transport in oxalate homeostasis. Semin Nephrol. 2008;28:143–51.
11. Chmiel JA, Carr C, Stuivenberg GA, Venema R, Chanyi RM, Al KF, Giguere D, Say H, Akouris PP, Domínguez Romero SA, et al: New perspectives on an old grouping: The genomic and phenotypic variability of Oxalobacter formigenes and the implications for calcium oxalate stone prevention. Frontiers in Microbiology. 2022;13:1011102.
12. Kaufman DW, Kelly JP, Curhan GC, Anderson TE, Dretler SP, Preminger GM, Cave DR. Oxalobacter formigenes may reduce the risk of calcium oxalate kidney stones. J Am Soc Nephrol. 2008;19:1197–203.
13. Jiang J, Knight J, Easter LH, Neiberg R, Holmes RP, Assimos DG. Impact of dietary calcium and oxalate, and Oxalobacter formigenes colonization on urinary oxalate excretion. J Urol. 2011;186:135–9.
14. Miller AW, Dearing D. The metabolic and ecological interactions of oxalate-degrading bacteria in the Mammalian gut. Pathogens. 2013;2:636–52.
15. Al KF, Daisley BA, Chanyi RM, Bjazevic J, Razvi H, Reid G, Burton JP: Oxalate-Degrading Bacillus subtilis Mitigates Urolithiasis in a Drosophila melanogaster Model. mSphere. 2020;5:e00498–20.
16. Zampini A, Nguyen AH, Rose E, Monga M, Miller AW. Defining Dysbiosis in Patients with Urolithiasis. Sci Rep. 2019;9:5425.
17. Tang R, Jiang Y, Tan A, Ye J, Xian X, Xie Y, Wang Q, Yao Z, Mo Z. 16S rRNA gene sequencing reveals altered composition of gut microbiota in individuals with kidney stones. Urolithiasis. 2018;46:503–14.
18. Ticinesi A, Milani C, Guerra A, Allegri F, Lauretani F, Nouvenne A, Mancabelli L, Lugli GA, Turroni F, Duranti S, et al. Understanding the gut-kidney axis in nephrolithiasis: an analysis of the gut microbiota composition and functionality of stone formers. Gut. 2018;67:2097–106.
19. Magwira CA, Kullin B, Lewandowski S, Rodgers A, Reid SJ, Abratt VR. Diversity of faecal oxalate-degrading bacteria in black and white South African study groups: insights into understanding the rarity of urolithiasis in the black group. J Appl Microbiol. 2012;113:418–28.
20. Kim HN, Kim JH, Chang Y, Yang D, Joo KJ, Cho YS, Park HJ, Kim HL, Ryu S. Gut microbiota and the prevalence and incidence of renal stones. Sci Rep. 2022;12:3732.
21. Denburg MR, Koepsell K, Lee JJ, Gerber J, Bittinger K, Tasian GE. Perturbations of the Gut Microbiome and Metabolome in Children with Calcium Oxalate Kidney Stone Disease. J Am Soc Nephrol. 2020;31:1358–69.
22. Miller AW, Choy D, Penniston KL, Lange D. Inhibition of urinary stone disease by a multi-species bacterial network ensures healthy oxalate homeostasis. Kidney Int. 2019;96:180–8.
23. Suryavanshi MV, Bhute SS, Gune RP, Shouche YS. Functional eubacteria species along with trans-domain gut inhabitants favour dysgenic diversity in oxalate stone disease. Sci Rep. 2018;8:16598.
24. Suryavanshi MV, Bhute SS, Jadhav SD, Bhatia MS, Gune RP, Shouche YS. Hyperoxaluria leads to dysbiosis and drives selective enrichment of oxalate metabolizing bacterial species in recurrent kidney stone endures. Sci Rep. 2016;6:34712.
25. Stern JM, Moazami S, Qiu Y, Kurland I, Chen Z, Agalliu I, Burk R, Davies KP. Evidence for a distinct gut microbiome in kidney stone formers compared to non-stone formers. Urolithiasis. 2016;44:399–407.
26. Liu Y, Jin X, Hong HG, Xiang L, Jiang Q, Ma Y, Chen Z, Cheng L, Jian Z, Wei Z, et al. The relationship between gut microbiota and short chain fatty acids in the renal calcium oxalate stones disease. FASEB J. 2020;34:11200–14.

27. Wolfe AJ, Toh E, Shibata N, Rong R, Kenton K, Fitzgerald M, Mueller ER, Schreckenberger P, Dong Q, Nelson DE, Brubaker L. Evidence of uncultivated bacteria in the adult female bladder. J Clin Microbiol. 2012;50:1376–83.
28. Whiteside SA, Razvi H, Dave S, Reid G, Burton JP. The microbiome of the urinary tract–a role beyond infection. Nat Rev Urol. 2015;12:81–90.
29. Xie J, Huang JS, Huang XJ, Peng JM, Yu Z, Yuan YQ, Xiao KF, Guo JN. Profiling the urinary microbiome in men with calcium-based kidney stones. BMC Microbiol. 2020;20:41.
30. Barr-Beare E, Saxena V, Hilt EE, Thomas-White K, Schober M, Li B, Becknell B, Hains DS, Wolfe AJ, Schwaderer AL. The Interaction between Enterobacteriaceae and Calcium Oxalate Deposits. PLoS ONE. 2015;10: e0139575.
31. Dornbier RA, Bajic P, Van Kuiken M, Jardaneh A, Lin H, Gao X, Knudsen B, Dong Q, Wolfe AJ, Schwaderer AL. The microbiome of calcium-based urinary stones. Urolithiasis. 2020;48:191–9.
32. Kachroo N, Monga M, Miller AW. Comparative functional analysis of the urinary tract microbiome for individuals with or without calcium oxalate calculi. Urolithiasis. 2022;50:303–17.
33. Jia G, Zhi A, Lai PFH, Wang G, Xia Y, Xiong Z, Zhang H, Che N, Ai L. The oral microbiota - a mechanistic role for systemic diseases. Br Dent J. 2018;224:447–55.
34. Palleja A, Mikkelsen KH, Forslund SK, Kashani A, Allin KH, Nielsen T, Hansen TH, Liang S, Feng Q, Zhang C, et al. Recovery of gut microbiota of healthy adults following antibiotic exposure. Nat Microbiol. 2018;3:1255–65.
35. Kuo C-L, Duan Y, Grady J: Unconditional or Conditional Logistic Regression Model for Age-Matched Case–Control Data? Frontiers in Public Health. 2018;6:57.
36. Al KF, Bisanz JE, Gloor GB, Reid G, Burton JP. Evaluation of sampling and storage procedures on preserving the community structure of stool microbiota: A simple at-home toilet-paper collection method. J Microbiol Methods. 2018;144:117–21.
37. Subar AF, Thompson FE, Kipnis V, Midthune D, Hurwitz P, McNutt S, McIntosh A, Rosenfeld S. Comparative validation of the Block, Willett, and National Cancer Institute food frequency questionnaires : the Eating at America's Table Study. Am J Epidemiol. 2001;154:1089–99.
38. Al KF, Burton JP. Processing human urine and ureteral stents for 16S rRNA amplicon sequencing. STAR Protoc. 2021;2: 100435.
39. Al KF, Denstedt JD, Daisley BA, Bjazevic J, Welk BK, Pautler SE, Gloor GB, Reid G, Razvi H, Burton JP. Ureteral Stent Microbiota Is Associated with Patient Comorbidities but Not Antibiotic Exposure. Cell Rep Med. 2020;1: 100094.
40. McDonald D, Hyde E, Debelius JW, Morton JT, Gonzalez A, Ackermann G, Aksenov AA, Behsaz B, Brennan C, Chen Y, et al. American Gut: an Open Platform for Citizen Science Microbiome Research. mSystems. 2018;3:e00031-00018.
41. Amir A, McDonald D, Navas-Molina JA, Debelius J, Morton JT, Hyde E, Robbins-Pianka A, Knight R: Correcting for Microbial Blooms in Fecal Samples during Room-Temperature Shipping. mSystems. 2017;2:e00199–16.
42. Parada AE, Needham DM, Fuhrman JA. Every base matters: assessing small subunit rRNA primers for marine microbiomes with mock communities, time series and global field samples. Environ Microbiol. 2016;18:1403–14.
43. Martin M. Cutadapt removes adapter sequences from high-throughput sequencing reads. 2011;2011(17):3.
44. Callahan BJ, McMurdie PJ, Rosen MJ, Han AW, Johnson AJ, Holmes SP. DADA2: High-resolution sample inference from Illumina amplicon data. Nat Methods. 2016;13:581–3.
45. Quast C, Pruesse E, Yilmaz P, Gerken J, Schweer T, Yarza P, Peplies J, Glockner FO. The SILVA ribosomal RNA gene database project: improved data processing and web-based tools. Nucleic Acids Res. 2013;41:D590-596.
46. Davis NM, Proctor DM, Holmes SP, Relman DA, Callahan BJ. Simple statistical identification and removal of contaminant sequences in marker-gene and metagenomics data. Microbiome. 2018;6:226.
47. Douglas GM, Maffei VJ, Zaneveld JR, Yurgel SN, Brown JR, Taylor CM, Huttenhower C, Langille MGI. PICRUSt2 for prediction of metagenome functions. Nat Biotechnol. 2020;38:685–8.
48. Sun S, Jones RB, Fodor AA. Inference-based accuracy of metagenome prediction tools varies across sample types and functional categories. Microbiome. 2020;8:46.
49. Andrews S: FastQC: A Quality Control Tool for High Throughput Sequence Data. 2010. http://www.bioinformatics.babraham.ac.uk/projects/fastqc.
50. Bolger AM, Lohse M, Usadel B. Trimmomatic: a flexible trimmer for Illumina sequence data. Bioinformatics. 2014;30:2114–20.
51. Langmead B, Salzberg SL. Fast gapped-read alignment with Bowtie 2. Nat Methods. 2012;9:357–9.
52. Mitchell AL, Almeida A, Beracochea M, Boland M, Burgin J, Cochrane G, Crusoe MR, Kale V, Potter SC, Richardson LJ, et al. MGnify: the microbiome analysis resource in 2020. Nucleic Acids Res. 2020;48:D570–8.
53. Kang DD, Froula J, Egan R, Wang Z. MetaBAT, an efficient tool for accurately reconstructing single genomes from complex microbial communities. PeerJ. 2015;3: e1165.
54. Parks DH, Imelfort M, Skennerton CT, Hugenholtz P, Tyson GW. CheckM: assessing the quality of microbial genomes recovered from isolates, single cells, and metagenomes. Genome Res. 2015;25:1043–55.
55. Olm MR, Brown CT, Brooks B, Banfield JF. dRep: a tool for fast and accurate genomic comparisons that enables improved genome recovery from metagenomes through de-replication. ISME J. 2017;11:2864–8.
56. Asnicar F, Thomas AM, Beghini F, Mengoni C, Manara S, Manghi P, Zhu Q, Bolzan M, Cumbo F, May U, et al. Precise phylogenetic analysis of microbial isolates and genomes from metagenomes using PhyloPhlAn 3.0. Nat Commun. 2020;11:2500.
57. Beghini F, McIver LJ, Blanco-Miguez A, Dubois L, Asnicar F, Maharjan S, Mailyan A, Manghi P, Scholz M, Thomas AM, et al: Integrating taxonomic, functional, and strain-level profiling of diverse microbial communities with bioBakery 3. Elife. 2021;10:e65088.
58. Murray JF Jr, Nolen HW 3rd, Gordon GR, Peters JH. The measurement of urinary oxalic acid by derivatization coupled with liquid chromatography. Anal Biochem. 1982;121:301–9.
59. Maalouf NM, Adams Huet B, Pasch A, Lieske JC, Asplin JR, Siener R, Hesse A, Nuoffer JM, Frey FJ, Knight J, et al. Variability in urinary oxalate measurements between six international laboratories. Nephrol Dial Transplant. 2011;26:3954–9.
60. Shen Y, Luo X, Li H, Guan Q, Cheng L. Evaluation of a high-performance liquid chromatography method for urinary oxalate determination and investigation regarding the pediatric reference interval of spot urinary oxalate to creatinine ratio for screening of primary hyperoxaluria. J Clin Lab Anal. 2021;35: e23870.
61. Nearing JT, Douglas GM, Hayes MG, MacDonald J, Desai DK, Allward N, Jones CMA, Wright RJ, Dhanani AS, Comeau AM, Langille MGI. Microbiome differential abundance methods produce different results across 38 datasets. Nat Commun. 2022;13:342.
62. Fernandes AD, Macklaim JM, Linn TG, Reid G, Gloor GB. ANOVA-like differential expression (ALDEx) analysis for mixed population RNA-Seq. PLoS ONE. 2013;8: e67019.
63. Morgan XC, Tickle TL, Sokol H, Gevers D, Devaney KL, Ward DV, Reyes JA, Shah SA, LeLeiko N, Snapper SB, et al. Dysfunction of the intestinal microbiome in inflammatory bowel disease and treatment. Genome Biol. 2012;13:R79.
64. vegan: Community Ecology Package. R package version 2.5–6 [https://CRAN.R-project.org/package=vegan].
65. Team RC. R: A language and environment for statistical computing. Vienna, Austria: In R Foundation for Statistical Computing; 2019.
66. Maaslin2: Maaslin2 [{http://huttenhower.sph.harvard.edu/maaslin2].
67. Gloor GB, Reid G. Compositional analysis: a valid approach to analyze microbiome high-throughput sequencing data. Can J Microbiol. 2016;62:692–703.
68. Gloor GB, Macklaim JM, Pawlowsky-Glahn V, Egozcue JJ. Microbiome Datasets Are Compositional: And This Is Not Optional. Front Microbiol. 2017;8:2224.
69. Mandal S, Van Treuren W, White RA, Eggesbo M, Knight R, Peddada SD. Analysis of composition of microbiomes: a novel method for studying microbial composition. Microb Ecol Health Dis. 2015;26:27663.

70. Lin H, Peddada SD. Analysis of compositions of microbiomes with bias correction. Nat Commun. 2020;11:3514.
71. Palarea-Albaladejo J, Martín-Fernández JA. zCompositions — R package for multivariate imputation of left-censored data under a compositional approach. Chemom Intell Lab Syst. 2015;143:85–96.
72. Letunic I, Bork P. Interactive Tree Of Life (iTOL) v5: an online tool for phylogenetic tree display and annotation. Nucleic Acids Res. 2021;49:W293–6.
73. Rivera-Pinto J, Egozcue JJ, Pawlowsky-Glahn V, Paredes R, Noguera-Julian M, Calle ML, Lozupone C. Balances: a new perspective for microbiome analysis. mSystems. 2018;3:e00053-00018.
74. Peschel S, Muller CL, von Mutius E, Boulesteix AL, Depner M: NetCoMi: network construction and comparison for microbiome data in R. Brief Bioinform. 2021;22:bbaa290.
75. Kortman GA, Raffatellu M, Swinkels DW, Tjalsma H. Nutritional iron turned inside out: intestinal stress from a gut microbial perspective. FEMS Microbiol Rev. 2014;38:1202–34.
76. Shen X, Yang Y, Li P, Luo H, Kong Q. Advances in the research of enterobacterial common antigen. Sheng Wu Gong Cheng Xue Bao. 2021;37:1081–91.
77. Dos Santos CA, Hernandes RT, Cunha MPV, Nagamori FO, Goncalves CR, Sacchi CT, Tiba-Casas MR, Camargo CH. Two Novel Mutations Associated with Polymyxin-B Resistance in a Pandemic Lineage of Uropathogenic Escherichia coli of the Sequence Type 69. Chemotherapy. 2021;66:92–8.
78. Das B, Bhadra RK. (p)ppGpp Metabolism and Antimicrobial Resistance in Bacterial Pathogens. Front Microbiol. 2020;11: 563944.
79. Percudani R, Peracchi A. The B6 database: a tool for the description and classification of vitamin B6-dependent enzymatic activities and of the corresponding protein families. BMC Bioinformatics. 2009;10:273.
80. Williams HE, Smith LH Jr. Disorders of oxalate metabolism. Am J Med. 1968;45:715–35.
81. Chmiel JA, Stuivenberg GA, Al KF, et al. Vitamins as regulators of calcium-containing kidney stones — new perspectives on the role of the gut microbiome. Nat Rev Urol. 2023;20:615–37. https://doi.org/10.1038/s41585-023-00768-5.
82. Van den Broeck T, Crul B, Heesakkers JP. Neurogenic voiding dysfunction induced by vitamin B6 overdose. Continence Reports. 2022;1:100004. https://doi.org/10.1016/j.contre.2022.100004.
83. Clark DJ. Adverse response to vitamin B6 in a 43 year old woman. Front Neurol. 2018. Conference Abstract: International Symposium on Clinical Neuroscience 2018. https://doi.org/10.3389/conf.fneur.2018.60.00011.
84. Almeida A, Mitchell AL, Boland M, Forster SC, Gloor GB, Tarkowska A, Lawley TD, Finn RD. A new genomic blueprint of the human gut microbiota. Nature. 2019;568:499–504.
85. Rampelli S, Soverini M, D'Amico F, Barone M, Tavella T, Monti D, Capri M, Astolfi A, Brigidi P, Biagi E, et al: Shotgun Metagenomics of Gut Microbiota in Humans with up to Extreme Longevity and the Increasing Role of Xenobiotic Degradation. mSystems. 2020;5:e00124–20.
86. Villarreal-Chiu JF, Quinn JP, McGrath JW. The genes and enzymes of phosphonate metabolism by bacteria, and their distribution in the marine environment. Front Microbiol. 2012;3:19.
87. Zhong Q, Kobe B, Kappler U. Molybdenum Enzymes and How They Support Virulence in Pathogenic Bacteria. Front Microbiol. 2020;11: 615860.
88. Winter SE, Winter MG, Xavier MN, Thiennimitr P, Poon V, Keestra AM, Laughlin RC, Gomez G, Wu J, Lawhon SD, et al. Host-derived nitrate boosts growth of E. coli in the inflamed gut. Science. 2013;339:708–11.
89. Sabatino JA, Starin D, Tuchman S, Ferreira C, Regier DS. Elevated urine oxalate and renal calculi in a classic galactosemia patient on soy-based formula. JIMD Rep. 2019;49:7–10.
90. Gacesa R, Kurilshikov A, Vich Vila A, et al. Environmental factors shaping the gut microbiome in a Dutch population. Nature. 2022;604:732–9. https://doi.org/10.1038/s41586-022-04567-7.
91. Alexander M, Ang QY, Nayak RR, Bustion AE, Sandy M, Zhang B, Upadhyay V, Pollard KS, Lynch SV, Turnbaugh PJ. Human gut bacterial metabolism drives Th17 activation and colitis. Cell Host Microbe. 2022;30(17–30): e19.
92. Lurgi M, Thomas T, Wemheuer B, Webster NS, Montoya JM. Modularity and predicted functions of the global sponge-microbiome network. Nat Commun. 2019;10:992.
93. Goncheva MI, Flannagan RS, Heinrichs DE: De Novo Purine Biosynthesis Is Required for Intracellular Growth of Staphylococcus aureus and for the Hypervirulence Phenotype of a purR Mutant. Infect Immun. 2020;88:e00104–20.
94. Jiang L, Zhao J, Guo R, Li J, Yu L, Xu D. Functional characterization and virulence study of ADE8 and GUA1 genes involved in the de novo purine biosynthesis in Candida albicans. FEMS Yeast Res. 2010;10:199–208.
95. Daisley BA, Koenig D, Engelbrecht K, Doney L, Hards K, Al KF, Reid G, Burton JP. Emerging connections between gut microbiome bioenergetics and chronic metabolic diseases. Cell Rep. 2021;37: 110087.
96. Liu M, Koh H, Kurtz ZD, Battaglia T, PeBenito A, Li H, Nazzal L, Blaser MJ. Oxalobacter formigenes-associated host features and microbial community structures examined using the American Gut Project. Microbiome. 2017;5:108.
97. Prokopovich S, Knight J, Assimos DG, Holmes RP. Variability of Oxalobacter formigenes and oxalate in stool samples. J Urol. 2007;178:2186–90.
98. Suryavanshi M, Agudelo J, Miller A. Rare phylotypes in stone, stool, and urine microbiomes are associated with urinary stone disease. Front Mol Biosci. 2023;10:1210225.
99. Holmes RP, Assimos DG. The impact of dietary oxalate on kidney stone formation. Urol Res. 2004;32:311–6.
100. Taylor EN, Curhan GC. Determinants of 24-hour urinary oxalate excretion. Clin J Am Soc Nephrol. 2008;3:1453–60.
101. Lee CR, Lee JH, Park M, Park KS, Bae IK, Kim YB, Cha CJ, Jeong BC, Lee SH. Biology of Acinetobacter baumannii: Pathogenesis, Antibiotic Resistance Mechanisms, and Prospective Treatment Options. Front Cell Infect Microbiol. 2017;7:55.
102. Looney WJ. Role of Stenotrophomonas maltophilia in hospital-acquired infection. Br J Biomed Sci. 2005;62:145–54 quiz 141 p following 154.
103. Perez-Carrasco V, Soriano-Lerma A, Soriano M, Gutierrez-Fernandez J, Garcia-Salcedo JA. Urinary Microbiome: Yin and Yang of the Urinary Tract. Front Cell Infect Microbiol. 2021;11: 617002.
104. Goneau LW, Hannan TJ, MacPhee RA, Schwartz DJ, Macklaim JM, Gloor GB, Razvi H, Reid G, Hultgren SJ, Burton JP: Subinhibitory antibiotic therapy alters recurrent urinary tract infection pathogenesis through modulation of bacterial virulence and host immunity. mBio. 2015;6:e00356–15.
105. Lemberger U, Pjevac P, Hausmann B, Berry D, Moser D, Jahrreis V, Özsoy M, Shariat SF, Veser J. The microbiome of kidney stones and urine of patients with nephrolithiasis. Urolithiasis. 2023;51:27.
106. Chutipongtanate S, Sutthimethakorn S, Chiangjong W, Thongboonkerd V. Bacteria can promote calcium oxalate crystal growth and aggregation. J Biol Inorg Chem. 2013;18:299–308.
107. Kanlaya R, Naruepantawart O, Thongboonkerd V: Flagellum Is Responsible for Promoting Effects of Viable Escherichia coli on Calcium Oxalate Crystallization, Crystal Growth, and Crystal Aggregation. Frontiers in Microbiology. 2019;10:2507.
108. El-Assmy A, Harraz AM, Eldemerdash Y, Elkhamesy M, El-Nahas AR, Elshal AM, Sheir KZ. Does lithotripsy increase stone recurrence? A comparative study between extracorporeal shockwave lithotripsy and non-fragmenting percutaneous nephrolithotomy. Arab J Urol. 2016;14:108–14.
109. Ozdedeli K, Cek M. Residual fragments after percutaneous nephrolithotomy. Balkan Med J. 2012;29:230–5.
110. Zhang X, Zhang D, Jia H, Feng Q, Wang D, Liang D, Wu X, Li J, Tang L, Li Y, et al. The oral and gut microbiomes are perturbed in rheumatoid arthritis and partly normalized after treatment. Nat Med. 2015;21:895–905.
111. Eberhard J, Stumpp N, Winkel A, Schrimpf C, Bisdas T, Orzak P, Teebken OE, Haverich A, Stiesch M. Streptococcus mitis and Gemella haemolysans were simultaneously found in atherosclerotic and oral plaques of elderly without periodontitis-a pilot study. Clin Oral Investig. 2017;21:447–52.
112. Chhibber-Goel J, Singhal V, Bhowmik D, Vivek R, Parakh N, Bhargava B, Sharma A. Linkages between oral commensal bacteria and atherosclerotic plaques in coronary artery disease patients. npj Biofilms and Microbiomes. 2016;2:7.
113. Fan X, Alekseyenko AV, Wu J, Peters BA, Jacobs EJ, Gapstur SM, Purdue MP, Abnet CC, Stolzenberg-Solomon R, Miller G, et al. Human oral

microbiome and prospective risk for pancreatic cancer: a population-based nested case-control study. Gut. 2018;67:120–7.
114. Momen-Heravi F, Babic A, Tworoger SS, Zhang L, Wu K, Smith-Warner SA, Ogino S, Chan AT, Meyerhardt J, Giovannucci E, et al. Periodontal disease, tooth loss and colorectal cancer risk: Results from the Nurses' Health Study. Int J Cancer. 2017;140:646–52.
115. Contaldo M, Fusco A, Stiuso P, Lama S, Gravina AG, Itro A, Federico A, Itro A, Dipalma G, Inchingolo F, et al: Oral Microbiota and Salivary Levels of Oral Pathogens in Gastro-Intestinal Diseases: Current Knowledge and Exploratory Study. Microorganisms. 2021;9:1064.
116. Siener R, Bangen U, Sidhu H, Honow R, von Unruh G, Hesse A. The role of Oxalobacter formigenes colonization in calcium oxalate stone disease. Kidney Int. 2013;83:1144–9.
117. Batagello CA, Monga M, Miller AW. Calcium Oxalate Urolithiasis: A Case of Missing Microbes? J Endourol. 2018;32:995–1005.
118. Kwak C, Kim HK, Kim EC, Choi MS, Kim HH. Urinary oxalate levels and the enteric bacterium Oxalobacter formigenes in patients with calcium oxalate urolithiasis. Eur Urol. 2003;44:475–81.
119. Heinken A, Khan MT, Paglia G, Rodionov DA, Harmsen HJ, Thiele I. Functional metabolic map of Faecalibacterium prausnitzii, a beneficial human gut microbe. J Bacteriol. 2014;196:3289–302.
120. Chen F, Bao X, Liu S, Ye K, Xiang S, Yu L, Xu Q, Zhang Y, Wang X, Zhu X, et al. Gut microbiota affect the formation of calcium oxalate renal calculi caused by high daily tea consumption. Appl Microbiol Biotechnol. 2021;105:789–802.
121. Duncan SH, Hold GL, Harmsen HJM, Stewart CS, Flint HJ. Growth requirements and fermentation products of Fusobacterium prausnitzii, and a proposal to reclassify it as Faecalibacterium prausnitzii gen. nov., comb. nov. Int J Syst Evol Microbiol. 2002;52:2141–6.
122. Peng L, Li ZR, Green RS, Holzman IR, Lin J. Butyrate enhances the intestinal barrier by facilitating tight junction assembly via activation of AMP-activated protein kinase in Caco-2 cell monolayers. J Nutr. 2009;139:1619–25.
123. Bashir M, Meddings J, Alshaikh A, Jung D, Le K, Amin R, Ratakonda S, Sharma S, Granja I, Satti M, et al. Enhanced gastrointestinal passive paracellular permeability contributes to the obesity-associated hyperoxaluria. Am J Physiol Gastrointest Liver Physiol. 2019;316:G1–14.
124. Liu Y, Jin X, Ma Y, Jian Z, Wei Z, Xiang L, Sun Q, Qi S, Wang K, Li H. Short-Chain Fatty Acids Reduced Renal Calcium Oxalate Stones by Regulating the Expression of Intestinal Oxalate Transporter SLC26A6. mSystems. 2021;6:e0104521.
125. Jin X, Jian Z, Chen X, Ma Y, Ma H, Liu Y, Gong L, Xiang L, Zhu S, Shu X, et al. Short Chain Fatty Acids Prevent Glyoxylate-Induced Calcium Oxalate Stones by GPR43-Dependent Immunomodulatory Mechanism. Front Immunol. 2021;12: 729382.
126. Dawson PA, Sim P, Mudge DW, Cowley D. Human SLC26A1 gene variants: a pilot study. ScientificWorldJournal. 2013;2013: 541710.
127. Finegold SM. Desulfovibrio species are potentially important in regressive autism. Med Hypotheses. 2011;77:270–4.
128. Konstantynowicz J, Porowski T, Zoch-Zwierz W, Wasilewska J, Kadziela-Olech H, Kulak W, Owens SC, Piotrowska-Jastrzebska J, Kaczmarski M. A potential pathogenic role of oxalate in autism. Eur J Paediatr Neurol. 2012;16:485–91.
129. Gupta A, Dhakan DB, Maji A, Saxena R, P KV, Mahajan S, Pulikkan J, Kurian J, Gomez AM, Scaria J, et al: Association of Flavonifractor plautii, a Flavonoid-Degrading Bacterium, with the Gut Microbiome of Colorectal Cancer Patients in India. mSystems. 2019;4:e00438–19.
130. Zeng X, Xi Y, Jiang W. Protective roles of flavonoids and flavonoid-rich plant extracts against urolithiasis: A review. Crit Rev Food Sci Nutr. 2019;59:2125–35.
131. Yamamoto S, Tsukamoto T, Terai A, Kurazono H, Takeda Y, Yoshida O. Genetic evidence supporting the fecal-perineal-urethral hypothesis in cystitis caused by Escherichia coli. J Urol. 1997;157:1127–9.
132. Tasian GE, Jemielita T, Goldfarb DS, Copelovitch L, Gerber JS, Wu Q, Denburg MR. Oral Antibiotic Exposure and Kidney Stone Disease. J Am Soc Nephrol. 2018;29:1731–40.
133. Khan SR. Reactive oxygen species, inflammation and calcium oxalate nephrolithiasis. Transl Androl Urol. 2014;3:256–76.

Publisher's Note